Heterogeneous Reaction of NO_2 on Hexane Soot: A Knudsen Cell and FT-IR Study

Hind A. Al-Abadleh and V. H. Grassian*

Departments of Chemistry and Chemical and Biochemical Engineering, The University of Iowa, Iowa City, Iowa 52242

Received: August 10, 2000; In Final Form: September 21, 2000

In this study, the reaction of NO_2 on freshly prepared hexane soot has been studied using a Knudsen cell reactor and FT-IR spectroscopy. Initial uptake coefficients were determined using gas-diffusion models that account for the surface area of the top layer of soot particles as well as the accessible underlying layers of soot particles. Under dry conditions, the initial uptake coefficient was found to be near 5×10^{-5} at a gas concentration of 2.5×10^{11} molecules cm^{-3} and a temperature of 295 K. In addition to reporting an initial uptake coefficient, uptake coefficients averaged over time and/or coverage are reported so as to compare to other values in the literature. Accounting for the increased surface area due to the underlying layers of soot particles, there is better agreement between the value of the uptake coefficient reported here using a Knudsen cell reactor and values determined from other experimental methods. The total amount of NO_2 reacted per unit surface area of soot and the conversion of NO_2 to HONO have been quantified. From these data, the atmospheric implication of the heterogeneous reaction of NO_2 on soot particles to form HONO is discussed.

Introduction

Heterogeneous reactions have been reported to be of some importance in the troposphere.[1] In particular, carbonaceous aerosol may provide a reactive surface for trace atmospheric gases including O_3,[2] SO_2,[3] and nitrogen oxides.[4−15] The heterogeneous reaction of ozone with soot aerosol has been investigated by Kamm et al.[2] They report that the kinetics of ozone decomposition on soot is complex and that ozone loss on soot particles may be nonnegligible in the polluted boundary layer, where the mass concentration of soot particles is extremely high. However, under most conditions in the troposphere and lower stratosphere, the reaction is of negligible importance. Recently, Koehler et al.[3] studied the heterogeneous uptake of SO_2 on *n*-hexane soot over the temperature range from −130 to −40 °C using FT-IR spectrometry. It was shown that there is rapid uptake of SO_2 on soot under dry conditions and low temperatures (−70 °C), similar to the conditions of the upper troposphere and lower stratosphere.

The heterogeneous reaction of nitrogen oxides, in particular NO_2, on carbonaceous aerosol has been studied by several groups using a variety of experimental techniques.[4−14] It has been shown that NO_2 can react with soot particles to produce HONO.[4−8] It has been proposed that this reaction may account for the high concentration of HONO observed during night time, when the homogeneous reaction, shown below, is insignificant:[16]

$$NO(g) + OH(g) \rightarrow HONO(g)$$

To assess the atmospheric importance of the heterogeneous reaction of NO_2 and soot, the kinetics of the reaction must be known. Most often a heterogeneous uptake coefficient, γ, is reported for surface reactions. The heterogeneous uptake coefficient, also referred to as a sticking coefficient, is defined as the ratio of the rate of molecules lost from the gas phase to the total gas−surface collision rate. Using a flow reactor, Longfellow et al.[4] reported that the uptake coefficient at 262 K, 27% relative humidity, and NO_2 gas concentration of 2×10^{11} molecules cm^{-3} to be in the range of $(2-4) \times 10^{-4}$ for propane and methane soot, 5×10^{-5} for kerosene soot, and 1×10^{-5} for hexane soot using the geometric surface area of the soot surface. In another study using a Knudsen cell reactor to measure the heterogeneous kinetics, the initial uptake coefficient for the reaction of NO_2 on ethylene soot was reported to be 0.095 ± 0.007 by Gerecke et al.[5] at 296 K using a NO_2 gas concentration of 7×10^{11} molecules cm^{-3}. The geometric area of the sample holder was used to determine the initial uptake coefficient in that study. The heterogeneous reaction of NO_2 on commercial and freshly prepared soot generated from the combustion of toluene, diesel, and kerosene was also investigated using a static reactor.[6] Mean uptake coefficients that accounted for the BET surface area of the commercial soot samples were determined to be $\sim 10^{-6}$ at 296 K for the consumption of 10^{13} NO_2 molecules cm^{-2} at a gas concentration of 25 ppm.

From the discussion above, it is clear that there is a range of values, from 0.095 to 10^{-6}, reported for the heterogeneous uptake coefficient of NO_2 on soot, a range that spans nearly 5 orders of magnitude. The discrepancy in the values of the uptake coefficient arises in part because the soot samples investigated were from different sources. Commercial soot differs from freshly prepared soot, and even the later can be prepared in different ways using different hydrocarbons. This means that from study to study soot particles can have different sizes, different BET surface areas, different chemical composition, and, therefore, different reactivities. Experimental conditions such as temperature, relative humidity, and pressure of NO_2 were also varied from one study to study.

Another source of discrepancy is that the accessible surface area for reaction must be accurately accounted for when calculating uptake coefficients. NO_2 may diffuse through the interparticle void areas and access underlying layers of particles.[6,17] However, in some of the above studies,[4,5,11] only uptake on the first layer of soot was considered, and thus, the exposed

* To whom correspondence should be addressed.

10.1021/jp002918i CCC: $19.00
Published on Web 12/01/2000

TABLE 1: Knudsen Cell Reactor Parameters

Reactor parameter	Value
Volume, V	964 cm^3
Total calculated surface area	1002 cm^2
Geometric area of the sample holder, A_s	11.95 cm^2
Effective area of the escape aperture,[a] $A_{h,eff}$	0.0677 cm^2
k_{esc} for NO_2	0.651 s^{-1} [b] ($\tau = 1.5$)[c]
	0.370 s^{-1} [d] ($\tau = 2.7$)[c]

[a] Effective area after accounting for the Claussing factor. [b] $k_{esc} = \bar{c}A_{h,eff}/4V$; $\bar{c} = (8RT/\pi M)^{1/2}$. [c] $\tau = 1/k_{esc}$. [d] k_{esc} experimentally determined.

geometric area of soot was used in calculating γ. This may explain the very high γ values reported in some studies compared to others. In addition, in all of the studies discussed above, surface areas were not measured for the soot samples under investigation. This is usually done using the BET method and N_2.[18] Instead, values were taken from the literature, which may or may not accurately represent the true values because of differences in sample preparation. The fractal nature of soot also makes the characterization of the available surface area difficult. As noted by Longfellow et al.,[4] in order to apply laboratory measurements of the heterogeneous uptake measurements to the atmosphere, the surface area of the soot must be considered.

Another difference in the literature values is that the initial uptake coefficient is reported in some cases, whereas a steady state or an average value is reported in others. This means that the reactivity of a surface covered with adsorbed molecules is compared to the reactivity of the unreacted surface. Because of site-blocking, adsorbate−adsorbate interactions, and electronic effects, uptake coefficients are typically coverage dependent and usually decrease as a function of coverage.[18,19]

In this study, the reaction of NO_2 with freshly prepared hexane soot has been studied using a Knudsen cell reactor and FT-IR spectroscopy. A limited number of experiments were done on toluene soot as well. The uptake coefficient for the NO_2·soot reaction was measured using a Knudsen cell reactor. Using models that take gas diffusion into account, an uptake coefficient that takes into consideration the accessible surface area and the increased number of gas surface collisions within the underlying layers is determined. We report here initial and average values of the uptake coefficient in order to compare to literature values. In addition, we have quantified gas-phase reactants and products in order to determine the total amount of NO_2 reacted with the soot surface as well as the branching of NO_2 uptake on the hexane soot surface to the production of HONO. FT-IR experiments were done in order to gain some additional insight into the heterogeneous reaction of NO_2 on soot and the possible role of adsorbed water that has been reported for this reaction.[4,6]

Experimental Section

A Knudsen cell reactor coupled to a quadruple mass spectrometer was used to study the kinetics of the uptake of NO_2 on hexane and toluene soot and to quantify gas-phase reactants and products. The reactor consists of a stainless steel cross that serves as the reaction chamber. The region between the reaction chamber and the mass spectrometer is separated by a gate valve and the escape aperture or escape hole. The size of the aperture can be changed in a vacuum using a linear-rotary motion feedthrough. The quadruple mass spectrometer (UTI, 100C) is pumped by a 150 L/s ion pump, and the region between the reactor and the mass spectrometer is pumped by a 70 L/s turbo pump (both from Varian). The stainless steel sample holder sits on top of a tee support in the reaction chamber and is O-ring sealed by a blank flange. Table 1 lists the Knudsen cell parameters used in this study. The most important parameters for the Knudsen cell are the escape constant, k_{esc}, and the residence time of the molecules inside the reactor, τ, where $\tau = 1/k_{esc}$.

When the sample compartment is opened to a steady-state flow of NO_2, loss of NO_2 to soot surface competes with escape through the exit aperture, causing a decrease in the mass spectrometer signal. Thus, the geometric uptake coefficient, γ_g, also referred to as the observed uptake coefficient, γ_{obs}, is determined from eq 1[20,21]

$$\gamma_g = \frac{A_{h,eff}}{A_s}\left(\frac{I_o - I}{I}\right) = \gamma_{obs} \qquad (1)$$

where $A_{h,eff}$ and A_s are listed in Table 1, I_o is the mass spectrometer signal for NO_2 prior to opening the sample compartment, and I is the mass spectrometer signal when the soot is exposed.

Freshly prepared samples of *n*-hexane or toluene soot were deposited directly on the sample holder by burning the vapor of about 30 mL of *n*-hexane (EM Science, purity 98.5%) or toluene (EM Science, purity 99.5%) in a small beaker. The sample was placed at a height of ∼5 cm from the top of the beaker so that soot is collected from the top part of the flame. Particle characterization studies of hexane and toluene soot were performed in order to have some insight about the nature of these particles. These characterization studies include particle size distribution analysis using transmission electron microscope images, specific BET surface areas, S_{BET}, and bulk density, ρ_b, measurements. Figure 1 shows representative TEM images of *n*-hexane soot and toluene soot. Table 2 lists the physical parameters of hexane and toluene soot. It should be noted that the size of the particles used here is close to the 30−50 nm diameter carbon particles found in aircraft exhaust.[22]

For the Knudsen cell experiments, soot samples were evacuated overnight to reach a pressure of $\sim 5 \times 10^{-8}$ Torr inside the reactor. The sample holder was then sealed and NO_2 (Matheson, 99.95% purity, used as received) was introduced to the reaction chamber through a leak valve to passivate the walls of the reactor. Experiments were run at NO_2 pressures near 8 μTorr (equivalent to 11 ppb or 2.5×10^{11} molecules cm^{-3}). The gas pressure inside the reaction chamber was monitored by an absolute pressure transducer (MKS 690 A.1TRC, range $0.1-10^{-6}$ Torr). All experiments were done at 295 K.

Prior to each experiment, calibration of pressure vs mass spectral intensity data for pure gaseous NO_2 ($m/e = 46$) was made. By using pure NO_2 for this calibration, the contribution of $^{15}NO_2$ ($m/e = 47$) to the $m/e = 47$ ion signal monitored during the course of the experiment can be calculated. The calibration of pure NO_2 also provides information about the fragmentation of NO_2 to NO ($m/e = 30$). Calibration of HONO is more difficult, since there is no readily available source of pure gaseous HONO. The mass spectrum of HONO shows a parent ion peak at $m/e = 47$ and two major fragments at $m/e = 17$ (OH^+) and $m/e = 30$ (NO^+); there is no apparent fragment at $m/e = 46$ (NO_2^+).[23] However, the parent ion peak ($m/e = 47$) has two contributions, the mass spectral intensity of $^{15}NO_2$ and HONO. Since the contribution of $^{15}NO_2$ to the $m/e = 47$ signal is known from the $^{14}NO_2$-signal, the mass spectral intensity of HONO can be determined. In addition, calibration of pure gaseous NO (Matheson, 99%) pressure versus mass spectral data of $m/e = 30$ ion signal was also done. The production of NO can be calculated by correcting for contributions to the ion

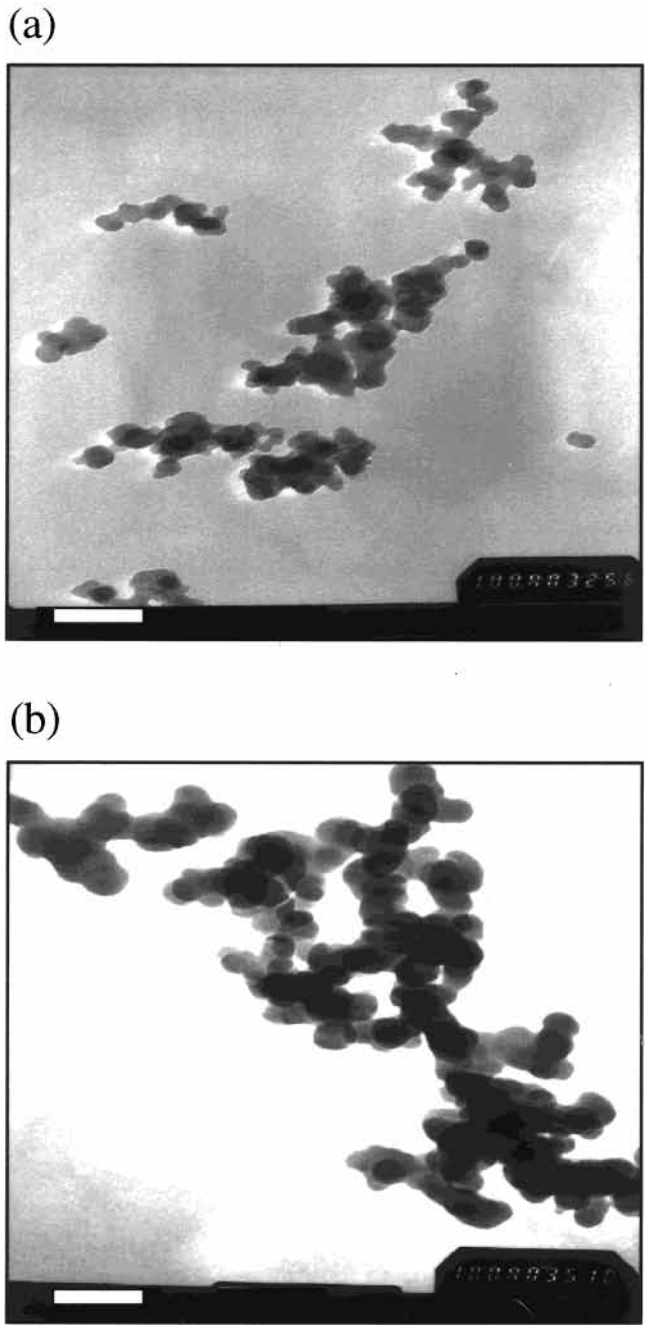

Figure 1. (a) TEM image of *n*-hexane soot taken at 100 000× magnification. (b) TEM image of toluene soot taken at 100 000× magnification. The bar in the left corner of each micrograph is equivalent to 100 nm.

TABLE 2: Physical Parameters of *n*-Hexane and Toluene Soot

Parameter	*n*-Hexane soot	Toluene soot
Particle diameter, nm	39 ± 13^a	58 ± 17
Bulk density, g cm^{-3}	$(13 \pm 6) \times 10^{-2}$	$(8 \pm 2) \times 10^{-2}$
Specific BET area, m^2 g^{-1}	76 ± 3	55 ± 5
True density,[b] g cm^{-3}	2.0	2.0

[a] The errors are $1 - \sigma$ statistical error. [b] Reference 27.

channel ($m/e = 30$) from fragmentation of NO_2 to NO. The fragmentation of HONO to NO is taken from the literature.[23] By using gas kinetic theory in conjunction with the experimentally determined cell parameters and calibration data, mass spectral intensities of ions can then be converted to flow (molecule s^{-1}) for the reactant molecule (NO_2) and product molecules (NO and HONO). Data were acquired every 0.5 s for each ion monitored during the course of the experiment.

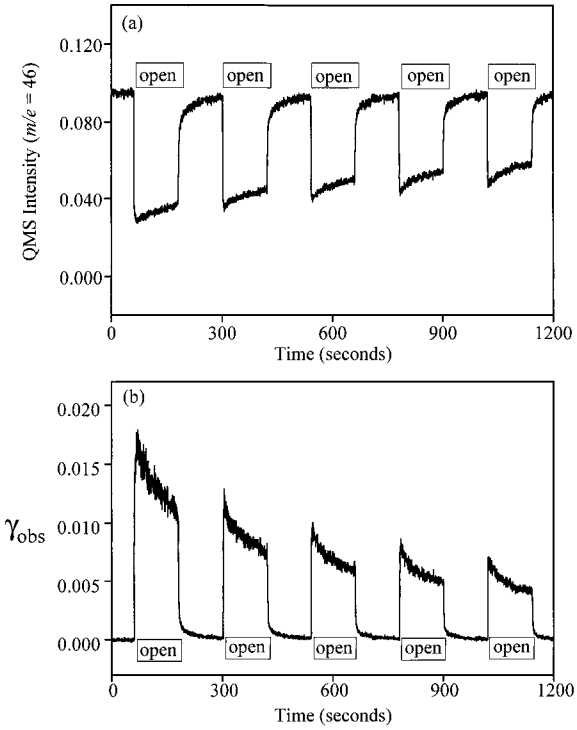

Figure 2. (a) Knudsen cell data for the heterogeneous uptake of NO_2 on soot (15.1 mg sample). The soot particles are exposed to NO_2 when the sample lid is open. The QMS intensity for $m/e = 46$ is shown. (b) Observed uptake coefficient calculated via eq 1 from the data shown in part a.

The IR cell used in this study has been modified from that previously described.[24] The new infrared cell now consists of a Teflon-coated stainless steel cube which is placed on a linear translator inside the sample compartment of the FT-IR spectrometer (Mattson RS-1, MCT narrow band detector). Freshly prepared hexane or toluene soot was deposited directly on half of a tungsten grid (3 cm × 2 cm) (Accumet Materials Co.). The grid is then mounted inside the IR cell and evacuated overnight. The linear translator allows each half of the sample grid to be scanned by the IR beam in order to obtain spectra of gas-phase and adsorbed reactants and products. Each spectrum was recorded by averaging 250 scans at an instrument resolution of 4 cm^{-1}. NO_2 pressures ranging from 5 to 100 mTorr (equivalent to 7−132 ppm or $(1.6-32.0) \times 10^{15}$ molecules/cm^3) were used in the FT-IR experiments. Distilled H_2O (Milli-Q) was subjected to several cycles of freeze−pump−thaw before use.

Results

A. Knudsen Cell Measurements for the Heterogeneous Uptake of NO_2 on Soot. Soot was directly deposited onto the Knudsen cell sample holder, which is 11.95 cm^2 in area. The initial uptake coefficient for the reaction of NO_2 with hexane soot was measured as a function of sample mass (and thus sample thickness). Representative Knudsen cell data are shown in Figure 2. The QMS intensity of NO_2 ($m/e = 46$) was monitored during the experiment (Figure 2a). When the sample lid is open and the soot particles are exposed to the reactive gas, there is a decrease in the QMS intensity. The QMS intensity of NO_2 is then converted to the observed uptake coefficient via eq 1, as shown in Figure 2b. The initial observed uptake coefficient, $\gamma_{o,obs}$, is taken as the maximum value for γ and found

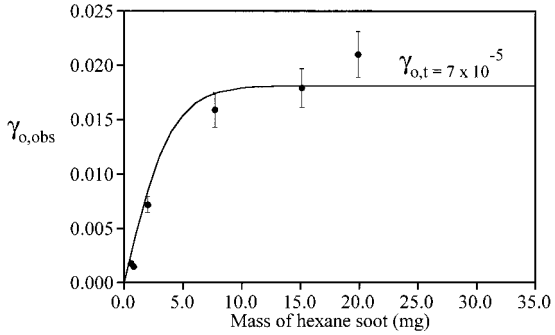

Figure 3. Mass dependence (thickness dependence) of the initial uptake coefficient for the reaction of NO_2 with hexane soot. Filled circles (●) represent experimental data, and the solid line (—) is a fit to the data that corrects for gas diffusion into the soot powder, giving a true initial uptake cofficient of 7×10^{-5} (see text for further details).

TABLE 3: Observed, BET, and Average Uptake Coefficient Values of NO_2 on *n*-Hexane Soot Using Different Experimental Conditions

Sample mass (mg)	$\gamma_{o,obs}$ ($\times 10^{-3}$)[a]	$\gamma_{o,BET}$ ($\times 10^{-5}$)[b]
0.6	1.80	4.72
0.8	1.50	2.95
2.0	7.22	5.68
7.7	15.9	3.25
15.1	17.9	1.86[c]
19.9	18.4	1.45[c]

[a] Calculated via eq 1. [b] Calculated via eq 3. [c] For these two samples, the masses were in the plateau region, so using the total BET area of these samples will result in a smaller uptake coefficient, because the entire BET area was not accessed by the gas-phase molecules.

to be 0.018 from the data shown in Figure 2. It can be seen from the data plotted in Figure 2 that over time the value of the uptake coefficient decreases as the reaction proceeds. This decrease occurs because the surface becomes less reactive with continued exposure of NO_2 and is interpreted as a coverage dependent uptake coefficient.

The value of the observed initial uptake coefficient was found to depend on the number of layers of soot present. The observed initial uptake coefficient measured as a function of the sample mass is plotted in Figure 3. Since the sample holder is of a fixed area, 11.95 cm^2, increasing the sample mass increases the number of layers of soot. The line through the data is determined from the gas diffusion model that Keyser et al. adapted from the catalysis area[25] to atmospherically relevant heterogeneous reactions.[26] This is a semiempirical model that accounts for gas diffusion into porous samples and corrects the observed uptake coefficient for contribution from underlying layers of particles. The parameters listed in Table 2 were used as input data in the diffusion model for the reaction of NO_2 with hexane soot. There are two parameters that are adjusted in order to obtain a good fit: the true initial uptake coefficient, $\gamma_{o,t}$, which takes into account the accessible surface area of the underlying layers, and the tortuosity, τ, which is related to the diffusion of the molecules through the sample. A value of 1 for the tortuosity and a value of 7×10^{-5} for the true initial uptake gave the best fit to the data.

A limited number of experiments was done on toluene soot. Initial uptake coefficient values of NO_2 on toluene soot were lower than those measured for hexane soot by a factor of 4.

As discussed in Underwood et al.,[28] there are two distinct regions in the plot shown in Figure 3. The region that extends from 0 to approximately 8 mg shows that the observed initial uptake coefficient has a nearly linear dependence on sample mass. The portion of the plot above 8 mg shows that the observed initial uptake coefficient is independent of the sample mass. The region above 8 mg shows that the probe depth of the gas-phase molecules measured during this initial time is constant and equivalent to the probe depth reached for a sample mass of 8 mg. In other words, on the time scale of the measurement of the initial uptake coefficient, NO_2 molecules are diffusing into only a portion of the soot sample estimated to be on the order of 1000 layers. For thin samples, the time scale for the observed uptake coefficient to reach its maximum value is on the order of the residence time (approximately 2 s). For a sample mass of 7.7 mg, this time scale is slightly longer, on the order of 3.5 s for the molecules to diffuse through all of the underlying layers. The diffusion constant can then be calculated from these data, the measured soot density, and eq 2[29]

$$l = (2Dt)^{1/2} \tag{2}$$

where l is the root-mean-square of the distance traveled, D is the diffusion constant, and t is the time. The parameter l can be determined from the sample mass where the plateau region begins (taken as 7.7 mg) using the geometric area of the sample holder and the experimentally determined density of the soot material (given in Table 2). The parameter t is taken as the experimentally determined time for γ to reach its maxiumum value (i.e. $t = 3.5$ s) at the plateau region. Using a value of $l = 5.0 \times 10^{-3}$ cm and a time of 3.5 s, the diffusion constant for NO_2 in hexane soot is calculated to be 3.5×10^{-6} cm^2/s.

Table 3 shows the initial observed uptake coefficient for each of the masses shown in Figure 3 along with an initial uptake coefficient that has been recalculated using the entire BET area of the soot samples according to eq 3:[28]

$$\gamma_{o,BET} = \gamma_{o,obs} \times \frac{A_S}{A_{BET}} \tag{3}$$

Using the entire BET area is an overcorrection for samples that are above ~8 mg as not all of the surface area is being accessed by the NO_2 molecules during the time scale of the measurement of the initial uptake coefficient. Indeed after correcting for the entire BET surface area, the two lowest values obtained are for the two samples whose masses are above 8 mg. The average of the first four values of $\gamma_{o,BET}$ is 4.2×10^{-5}.

For the same experimental data shown in Figure 3, average observed uptake coefficients were calculated over a 140 s time period. The data plotted in Figure 4 show $\gamma_{ave,obs}$ as a function of mass of *n*-hexane soot. It is seen that $\gamma_{ave,obs}$ is a linear function of sample mass over the entire range. The average uptake coefficient can be corrected for the accessible BET area using a linear least-squares fit of the line through the data points. This correction is then obtained from eq 4:

$$\gamma_{ave,BET} = \text{slope } (mg^{-1}) \times \frac{A_S\ (cm^2)}{S_{BET}\ (cm^2 mg^{-1})} \tag{4}$$

The slope of the line in Figure 4 is 7.7×10^{-4} mg^{-1} and the value of γ_t calculated using eq 3 is 1.2×10^{-5}. This is a factor of 6 times lower than the true initial value of the uptake coefficient. Although the application of the diffusion model in Figure 3 predicts a nearly linear mass regime to be in the range from 0 to 8 mg for the initial uptake coefficient, the dependence of the average uptake coefficient on the mass is still linear up to 19 mg, as shown in Figure 4. The linear region for any time-averaged uptake coefficient can be predicted from the diffusion

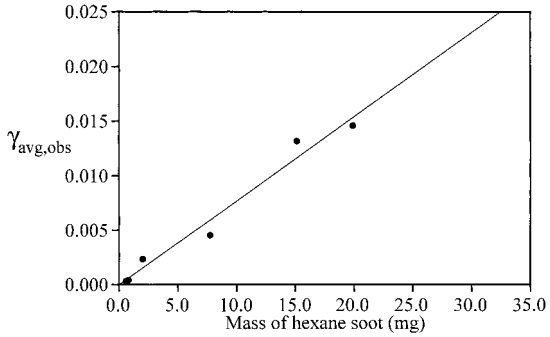

Figure 4. Linear mass dependence of the average uptake coefficient, averaged over 140 seconds. Filled circles (●) represent experimental data, and the solid line (−) represents a linear least-squares fit to the data of the form $y = mx$. The slope of the fit is 7.7×10^{-4} mg^{-1}, with an R value of 0.986.

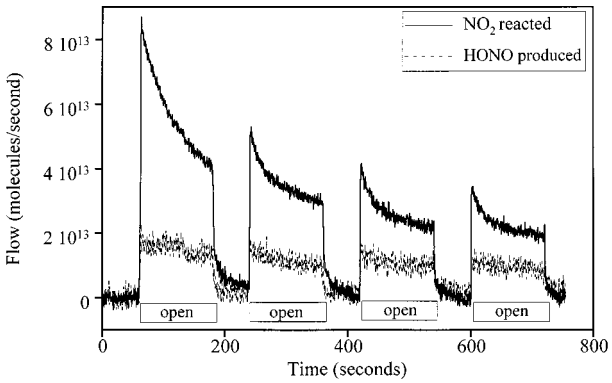

Figure 5. Calibrated flow of NO_2 reacted and HONO produced (7.7 mg sample).

constant determined above, i.e., $l = [2 \times (3.5 \times 10^{-6}\ \text{cm}^2/\text{s}) \times 140]^{1/2} = 3.2 \times 10^{-2}$ cm. It is predicted that, in a 140 s period, the uptake coefficient would be linear up to a diffusion length of 3.1×10^{-2} cm. From the soot density of 0.13 g/cm^3 and sample geometric area this diffusion length is equivalent to a mass of 48 mg. These data show that NO_2 molecules can access additional underlying layers of the soot sample over time and that the probe depth of NO_2 through the powdered sample increases with time.

In some experiments, the parent peak of HNO_3 ($m/e = 63$) was monitored. No change in the mass spectral intensity of HNO_3 was observed, suggesting that HNO_3 is not formed as a gaseous reaction product. This result agrees with the study of Kalberer et al.,[7] in which HNO_3 was not detected either in the gas phase or adsorbed on the aerosol particles or the walls of the reactor. The HONO mass channel ($m/e = 47$) was also monitored. There was an increase in the $m/e = 47$ signal as NO_2 reacted with the surface. Quantification of the HONO production is described below.

B. Calibrated Flow Experiments Used To Determine the Branching of NO_2 to HONO and the Total Uptake. The QMS intensity for the parent ions of NO_2 and HONO, $m/e = 46$ and 47, respectively, were calibrated and converted to molecular flow through the Knudsen cell. These data are shown in Figure 5. The flow of NO_2 has been offset and inverted to show the amount of NO_2 that reacts per second. Since the $m/e = 47$ signal from the mass spectrometer contains two contributions: the parent ions of HONO and the natural abundance ^{15}N-labeled NO_2. Calibration of the $m/e = 47$ signal for HONO production was done according to the procedure outlined in the Experimental Section. From the calibrated data presented in Figure 5, the amount of HONO produced per NO_2 reacted is determined to be 36 ± 5%. The remaining NO_2 taken to the surface may correspond to the formation of surface-bound products (vide infra) and other gas products such as NO. The percentage of HONO produced in this study is lower than that reported in another Knudsen cell study.[5] This may be a result of using a different hydrocarbon as a soot generator and collecting soot at different heights from the flame base both of which has been shown to effect HONO production.[4,5]

TABLE 4: Values of the Uptake Coefficient

(a) Initial and at Specific Surface Coverages

Mass of soot (mg)	BET surface area (cm^2)	$\gamma_{o,BET}$ ($\times 10^{-5}$)	$\gamma_{0.1,BET}$ ($\times 10^{-5}$)	$\gamma_{0.25,BET}$ ($\times 10^{-5}$)	$\gamma_{0.50,BET}$ ($\times 10^{-5}$)
0.6	456	4.72	1.00	0.31	*a*
0.8	608	2.95	1.26	0.73	0.42
2.0	1520	5.68	1.01	0.44	*a*
7.7	5852	3.25	0.37	0.22	*a*
15.1	11476	1.86	1.12	0.76	0.32
19.9	15124	1.66	0.82	0.48	0.33

(b) Averaged over Time And Surface Coverages

Mass of soot (mg)	$\gamma_{ave,BET}$ ($\times 10^{-5}$)				
	at 140 s	at 300 s	0.1 coverage[b]	0.25[b]	0.50[b]
0.6	0.83	0.74	1.41	0.69	*a*
0.8	0.84	0.51	1.77	1.17	0.69
2.0	1.86	1.03	1.72	0.76	*a*
7.7	0.93	0.58	0.80	0.48	*a*
15.1	1.37	1.00	1.37	0.99	0.71
19.9	1.15	.99	1.03	0.76	0.60

[a] Some experiments were ended before a coverage of 0.50 was reached. [b] Surface coverage values of 0.1, 0.25, 0.5 were calculated using the maxim coverage of NO_2 on soot, which under the conditions of this study (pressure of 8 μTorr) is taken as 1.4×10^{13} molecules cm^{-2}.

From the calibrated data it is also possible to determine the absolute number of NO_2 molecules reacted per unit surface area (or unit mass of soot). For small masses of soot (<1 mg), complete saturation of the surface can be obtained by continuing the reaction until no further uptake of NO_2 is observed. This means that over time the uptake coefficient goes to zero. The data in Figure 5 can be used to determine the total amount of NO_2 reacted per unit surface area. For thin or low mass samples, complete saturation occurs over the time period of the experiment, whereas for thicker samples with larger mass, the data are fit to a double exponential form, and the fit is then extrapolated to the limit of no further uptake of NO_2 corresponding to a saturated surface. From all of the data, it is determined that the total amount of NO_2 that can react at a pressure near 8 μTorr is determined to be $(1.4 \pm 0.5) \times 10^{13}$ molecules cm^{-2}. This value is used as a saturation coverage for NO_2 on soot at 295 K and a pressure of 8 μTorr.

Using a saturation coverage of 1.4×10^{13} molecules cm^{-2}, the uptake coefficient can be calculated at specific coverages. These data are presented in Table 4, which lists initial uptake coefficients and those determined for NO_2 coverages of one-tenth, one-quarter, and one-half (0.1, 0.25 and 0.5) of the saturation coverage, which corresponds to 1.4×10^{12}, 3.5×10^{12}, and 7×10^{12} molecules cm^{-2}, respectively. All of the numbers reported in Table 4 have been corrected for the entire BET area of the soot sample. It is seen from the data for a specified mass of soot that γ decreases as the coverage of NO_2 increase. The reaction of NO_2 with soot is not catalytic under the conditions used in the study, and therefore active sites are either blocked by reaction products from irreversible NO_2 adsorption or from chemical deactivation.

For one set of experimental data, the variation of γ_{BET} with

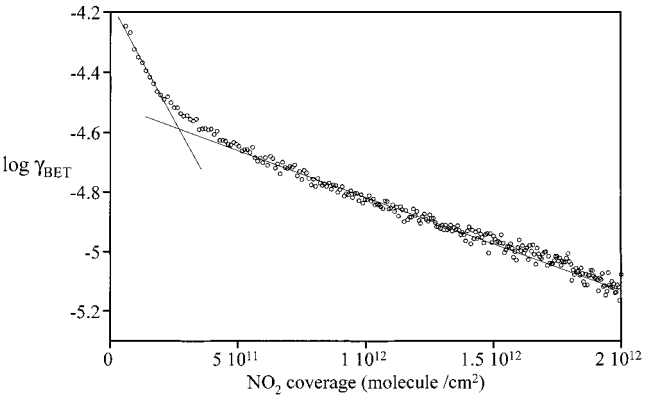

Figure 6. Log of γ_{BET} versus NO_2 coverage. At low coverage of NO_2, the data fits the linear equation $y = -4.18 - (1.46 \times 10^{-12})x$. At higher coverages of NO_2, data fits the linear equation $y = -4.52 - (2.96 \times 10^{-13})x$.

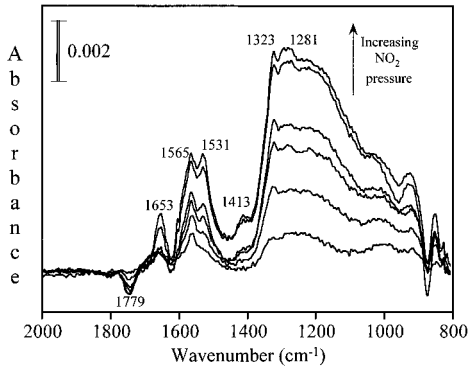

Figure 7. FT-IR spectra of hexane soot surface recorded as a function of NO_2 pressure (5, 11, 23, 46, 63, and 91 mTorr). Spectra were recorded in the presence of gas-phase NO_2 (gas-phase absorptions were subtracted out).

NO_2 coverage was determined in order to further understand the coverage dependence of γ. Figure 6 shows a plot the log of γ_{BET} as a function of NO_2 coverage in molecules cm^{-2}. The data can be fit to two straight lines corresponding to a double exponential fit. At low coverages of NO_2, the linear least-squares fit of the data is $y = -4.18 - (1.46 \times 10^{-12})x$. However, at higher coverages of NO_2, data fits the linear equation $y = -4.52 - (2.96 \times 10^{-13})x$. It is not clear what the exact fundamental nature of the coverage dependence is due to. This type of coverage dependence may be explained by several reasons,[18,19] including surface site heterogeneity and repulsive adsorbate−adsorbate interactions. As will be discussed in the next section, adsorbed NO_2 does remain on the surface of the soot particles.

C. FT-IR Study of the Heterogeneous Reaction of NO_2 on Soot. Figure 7 shows the FT-IR spectra of hexane soot (1 mg) as a function of NO_2 pressure. FT-IR experiments were done at higher pressures (ppm) than the Knudsen cell experiments, because of the lower sensitivity of the technique. The infrared spectra recorded as a function of increasing pressure of NO_2 from 5 to 91 mTorr are shown in Figure 7. These spectra were recorded in the presence of gas-phase NO_2; the unreacted soot surface was taken as the reference background spectrum. The spectra showing only surface-bound products are obtained by spectral subtraction of gas-phase absorptions. The intensity of the bands at 1281, 1323, 1531, 1565, and 1653 cm^{-1} increase as the coverage of NO_2 is increased. There is a decrease in the intensity of the band at 1779 cm^{-1}, suggesting the loss of the C═O group from the carbonyl surface, presumably due to the formation of gas-phase CO_2 or CO, as has been observed in other studies done at high pressures of NO_2.[14] Upon evacuation of the gas phase, the infrared spectrum of the surface remains nearly identical, with only a small decrease in intensity of the bands between 1400 and 1675 cm^{-1}. On the basis of literature assignments, the absorptions bands of the surface-bound species can be assigned to different functional groups present on the soot surface after reaction with NO_2 (see Table 5).

TABLE 5: Assignment of Vibrational Bands of Surface Bound Species from the Adsorption of NO_2 on Hexane Soot

Surface species	Wavenumber (cm^{-1})
R−ONO	1281,[a] 1280[b]
R−NO_2	1323,[a] 1340[b,c]
CO_3^{2-} (ad)	1413[a]
R−NO_2	1531,[a] 1540[b,c]
R−N−NO_2	1565[a,b]
R−O−NO	1653,[a] 1660[c]
lactone and alkyl carbonyl groups	1779,[a] 1775[b]

[a] This work. [b] Reference 9. [c] Reference 13.

Several additional pressures of NO_2 were introduced into the infrared cell containing the soot sample until there was no longer any more changes in the surface spectrum. To try and reactivate the soot sample, the infrared cell was evacuated overnight and then 5.0 Torr of distilled H_2O was added to the infrared cell for 20 min, as water has been shown to reactivate the soot surface.[4,6] A spectrum of the surface—after evacuation of water—was compared to that before the addition of water to see if water caused a change to the surface or not. The bending mode of adsorbed H_2O at 1625 cm^{-1} was seen in the spectrum. After that, successive pressures of NO_2 were added to the surface in the same manner. Spectra of the surface were referenced to that after evacuation of H_2O. These spectra show an obvious decrease in the intensity of the 1625 and 1779 cm^{-1} bands due to the loss of H_2O and C═O groups from the surface after the addition of 52, 75, and 95 mTorr of NO_2. Addition of pressures of NO_2 less than 52 mTorr did not show bands of adsorbed NO_2 on the surface. HONO(g) bands[30] at 1264, 1703, and 3591 cm^{-1} were not observed in any of the gas-phase spectra recorded in the presence of NO_2. This may be a result of using a short IR path length, since relatively small amounts of HONO are produced from the reaction of NO_2 with hexane soot. However, the loss of water from the surface and the growth of the carbonate band at 1413 cm^{-1} suggests further oxidation of the surface.

Discussion

In two recent studies of the NO_2 reaction on soot aerosol, the analysis of the data obtained for the same reaction using a Knudsen cell reactor has been called into question.[6,17] This is because in Knudsen cell studies—often referred to as bulk studies—uptake coefficients are usually calculated using only the geometrical surface area of the sample holder.[5,11] Using the geometric area as the effective surface area for heterogeneous uptake may introduce a major under estimation of the available surface area for reaction. This will especially be true for small particles with high surface areas, such as soot. Soot is a porous material, and with its fractal geometry, a relatively large amount of surface area may be accessible for NO_2 to adsorb and react. In this study, initial uptake coefficient values calculated using the geometric area were corrected to take into account the diffusion of NO_2 into the interparticle pores of the soot sample and its ability to access underlying soot layers. By doing so the true value of the initial uptake is determined to be 7×10^{-5}, significantly lower than the value obtained using the geometric area.

TABLE 6: Comparison of Initial, Specific Coverage, and Average Uptake Coefficients

Uptake coefficient	Average values	Range of values
	Initial Uptake Coefficients	
$\gamma_{o,obs}$		$(1.8-18) \times 10^{-3}$
$\gamma_{o,BET}$	$(3.4 \pm 1.6) \times 10^{-5}$	$(1.5-5.7) \times 10^{-5}$
	Uptake Coefficients at Different Coverages	
$\gamma_{0.1,BET}$	$(9.3 \pm 0.3) \times 10^{-6}$	$(3.7-12.6) \times 10^{-6}$
$\gamma_{0.25,BET}$	$(4.9 \pm 0.2) \times 10^{-6}$	$(2.2-7.6) \times 10^{-6}$
$\gamma_{0.5,BET}$	$(3.6 \pm 0.6) \times 10^{-6}$	$(3.2-4.6) \times 10^{-6}$
	Time Averaged Uptake Coefficients[a]	
$\gamma_{ave,BET\ (140\ s)}$	$(1.2 \pm 0.4) \times 10^{-5}$	$(0.8-1.9) \times 10^{-5}$
$\gamma_{ave,BET\ (300\ s)}$	$(8.2 \pm 2.2) \times 10^{-6}$	$(5.1-10.3) \times 10^{-6}$
	Coverage Averaged Uptake Coefficients[b]	
$\gamma_{ave,BET\ (0.1)}$	$(1.4 \pm 0.4) \times 10^{-5}$	$(0.8-1.8) \times 10^{-5}$
$\gamma_{ave,BET\ (0.25)}$	$(8 \pm 2) \times 10^{-6}$	$(5-11) \times 10^{-6}$
$\gamma_{ave,BET\ (0.5)}$	$(6.7 \pm 0.6) \times 10^{-6}$	$(6.0-7.1) \times 10^{-6}$

[a] Uptake coefficients averaged from time $t = 0$ to the indicated time. [b] Uptake coefficients averaged from a coverage of zero to the indicated coverage.

It is also typical to report initial uptake coefficients determined for very short reaction times in Knudsen cell experiments. In other measurements using aerosol chambers, flow reactors, and other static reactors, average or steady-state values are often reported. When γ_{ave} is reported in the literature, it corresponds to the reaction occurring over longer time scales. From study to study, uptake coefficients are averaged over different time scales and, therefore, over different surface coverages. Here we report γ_{BET} averaged over coverage. This is a more fundamental quantity for surface reactions than time since different soot samples of varying mass can reach the same coverage at different times. The major assumption made in this analysis is that the underlying layers and the top layers of the soot sample are reaching the same coverage at the same time, when in fact there may be a coverage gradient with the top layers being at higher coverages compared to the bottom most layers. Further analysis of the data would require detailed knowledge of saturation effects of NO_2 adsorbed on soot samples. An analysis of this type is currently underway.

Table 6 summarizes the uptake coefficients calculated in different ways (initial uptake coefficients determined using geometric and BET areas, uptake coefficients at specified coverages, and uptake coefficients averaged over coverage and time). Initial uptake coefficients corrected for the BET surface area of soot samples have a narrower range than the observed uptake coefficient using the sample holder geometric area. The coverage and time-average determined uptake coefficients are lower than the initial ones. The FT-IR data show that the surface becomes covered with adsorbed molecules as the reaction proceeds. Once the surface was covered, it was not possible to recover the reactivity of the soot particles.

The data generated in this study can be used to reexamine measurements made in other laboratories. The geometric uptake coefficient reported by Gerecke et al.[5] using a Knudsen cell reactor can be corrected for diffusion of NO_2 (see Table 7). They reported an initial uptake coefficient for NO_2 on ethlylene soot to be 0.095 ± 0.007. An 8.0 mg sample of soot reported in their study has a BET surface area of 6080 cm^2 (assuming that the BET surface area of ethylene soot equals 76 $m^2\ g^{-1}$). Using eq 3 with the geometric area of the sample holder equal to 19.6 cm^2, $\gamma_{o,BET}$ can be calculated to be about 3×10^{-4}, which is approximately a factor of 4 times greater than the initial uptake determined here of 7×10^{-5} using a gas-diffusion model.

TABLE 7: Uptake Coefficient Values Reported in the Literature Corrected for BET Surface Area

Soot	Mass (mg)	BET surface area ($m^2\ g^{-1}$)	Geometric uptake coefficient, γ_g	BET uptake coefficient, γ_{BET}
		a. Longfellow et al.[a]		
Methane	2.6	25	3.0×10^{-4}	2.5×10^{-5}
Propane	4.0	130	3.0×10^{-4}	3.2×10^{-6}
Hexane	1.0	89[a]	1.0×10^{-5}	6.2×10^{-7}
		76[b]		7.2×10^{-7}
Kerosene	2.1	na	5.0×10^{-5}	na[c]
		b. Gerecke et al.[d]		
Ethylene	8.0	76	9.5×10^{-2}	3.0×10^{-4}

[a] For Longfellow et al. study (ref 4), γ_{BET} was calculated using eq 3 with the geometric area of the flow reactor equal to 55 cm^2. The given BET surface area in Longfellow et al. was 89 m^2/g. [b] BET area determined in this study. [c] na: not available. [d] For Gerecke et al. study (ref 5), γ_{BET} was calculated using eq 3 with the geometric area of the sample holder equal to 19.6 cm^2.

The data averaged over time and coverage can be compared to some of the measurements made using different techniques. Longfellow et al.[4] studied the reaction of NO_2 on methane, propane, hexane, and kerosene soot using a flow reactor. Uptake coefficient values reported in their study are corrected for BET surface area in Table 7. It can be seen that the steady state γ_{BET} for the hexane soot is a factor of 10−20 times lower than the average (coverage and time) reported in Tables 4 and 6. This may be due to a temperature effect, since their experiments were done at 262 K.

Kleffmann et al.[6] studied the consumption of NO_2 on commercial soot samples with a well-characterized BET surface area. Mean uptake coefficient values were derived from the slopes of the first-order decay constants during the first 5 min of the reaction as a function of the BET surface area of the soot samples. Those γ values were determined to be $\sim 10^{-6}$ for the consumption of $\sim 10^{13}$ NO_2 cm^{-2}, close to the values that we obtain for hexane soot. In their study, uptake coefficient values were not determined for freshly prepared soot samples, because of the unavailability of the BET surface area values for these samples.

To determine the atmospheric significance of the reaction of NO_2 to yield HONO, the reactive uptake coefficient must be known. Under the dry conditions reported here, the initial reactive uptake coefficient would be the fraction of NO_2 converted to HONO times the measured uptake coefficient, i.e., $0.36 \times (7 \times 10^{-5}) = 2.5 \times 10^{-5}$. Atmospheric models to determine the importance of this reaction under atmospheric conditions would need to take into account the coverage dependence of the uptake coefficient and the fact that the surface becomes deactivated over time. Further analysis of this reaction would require additional experimentation under more atmospherically relevant conditions that span the temperature and relative humidity range of the troposphere.

Conclusions

In this study, the heterogeneous reaction of NO_2 with freshly prepared hexane soot has been studied using a Knudsen cell reactor and FT-IR spectroscopy at 295 K. The FT-IR data show that adsorbed products remain on the surface in agreement with another very recent FT-IR investigation of the NO_2 soot reaction.[31] HONO was detected as a gas-phase reaction product, accounting for 36% of the NO_2 reacted. Initial uptake coefficients were determined by accounting for the accessible surface area of the soot samples on the time scale of the measurement.

The time scale is on the order of the residence time of the gas molecules inside the Knudsen cell reactor. On this time scale, diffusion into the bulk powder can occur. Diffusion of gases into the bulk of the material may be important in other systems involving solid particle surfaces as well, thus making the geometric area inappropriate for use in determining the uptake coefficient. Uptake coefficients averaged over longer times and higher coverages were nearly an order of magnitude lower than the initial uptake coefficient. Comparison to values reported in the literature using other techniques are now in better agreement with the Knudsen cell data when the BET areas of the soot samples are considered and average values of the uptake coefficient are compared. This discrepancy was previously 5 orders of magnitude, making it difficult to fully assess the importance of the heterogeneous reaction of NO_2 on soot to form HONO in the atmosphere.

Acknowledgment. The authors gratefully acknowledge the Department of Energy-Atmospheric Chemistry Program for support of this work (DE-FG01-98ER62580).

References and Notes

(1) Noble, C. A.; Prather, K. A. *Phys. World* **1998**, *11*, 39.
(2) Kamm, S.; Möhler, O.; Naumann, K.-H.; Saathoff, H.; Schurath, U. *Atmos. Environ.* **1999**, *33*, 4651.
(3) Koehler, B. G.; Nicholson, V. T.; Roe, H. G.; Whitney, E. S. *J. Geophys. Res.* **1999**, *104-D5*, 5507.
(4) Longfellow, C. A.; Ravishankara, A. R.; Hanson, O. R. *J. Geophys. Res.* **1999**, *104-D11*, 13833.
(5) Gerecke, A.; Thielmann, A.; Gutzwiller, L.; Rossi, M. *Geophys. Res. Lett.* **1998**, *25*−*13*, 2453.
(6) Kleffmann, J.; Becker, K.; Lackhoff, M.; Wiesen, P. *Phys. Chem. Chem. Phys.* **1999**, *1*, 5443.
(7) Kalberer, M.; Ammann, M.; Arens, F.; Gäggeler, H. M.; Baltensperger, U. *J. Geophys. Res.* **1999**, *104-D11*, 13825.
(8) Ammann, M.; Kalberer, M.; Jost, D. T., Tolber, L.; Rössler, E.; Piguet, H. W.; Gäggeler, H. W.; Baltensperger, U. *Nature* **1998**, *395*, 157.
(9) Akhter, M. S.; Chughtai, A. R.; Smith, D. M. *J. Phys. Chem.* **1984**, *88*, 5334.
(10) Kalberer, M.; Ammann, M.; Gäggeler, H. M.; Baltensperger, U. *Atmos. Environ.* **1999**, *33*, 2815.
(11) Rogaski, C. A.; Golden, D. M.; Williams, L. R. *Geo. Phys. Res. Lett.* **1997**, *24*, 381.
(12) Kalberer, M.; Tabor, K.; Ammann, M.; Parrat, Y.; Weingarther, E.; Pighet, D.; Rössler, E.; Jost, D. T.; Türler, A.; Gäggeler, H. W.; Baltensperger, U. *J. Phys. Chem.* **1996**, *100*, 15487.
(13) Smith, D. M.; Welch, W. F.; Graham, S. M.; Chughtai, A. R.; Wicke, B. G.; Grady, K. A. *Appl. Spectrosc.* **1988**, *42*, 674.
(14) Chughtai, A. R.; Welch, W. F.; JR.; Akhter, M. S.; Smith, D. M. *Appl. Spectrosc.* **1990**, *44*, 294.
(15) Choi, W.; Leu, M.-T. *J. Phys. Chem. A.* **1998**, *102*, 7618.
(16) Harrison, R. M.; Peak, J. D.; Collins, G. M. *J. Geophys. Res.* **1996**, *101-D9*, 14429.
(17) Aumont, B.; Madronich, S.; Ammann, M.; Kalberer, M.; Baltensperger, U.; Hauglustaine, D.; Brocheton, F. *J. Geophys. Res.* **1999**, *104-D1*, 1729.
(18) Adamson, A. W. *Physical Chemistry of Surfaces*, 5th ed.; John Wiley & Sons: New York, 1990.
(19) Masel, R. *Principles of Adsorption and Reaction on Solid surfaces*; John Wiley & Sons: New York, 1996.
(20) Beichert, P.; Finlayson-Pitts, B. J. *J. Phys. Chem.* **1996**, *100*, 15218.
(21) Golden, D. M.; Spokes, G. M.; Benson, S. W. *Angew Chem., Ent. Ed. Engl.* **1973**, *12*, 534.
(22) Hagen, D. E.; Trueblood, M. B.; Whitefield, P. D. *Particulate Sci. Technol.* **1992**, *10*, 53.
(23) Fenter, F. F.; Caloz, F.; Rossi, M. J. *J. Phys. Chem.* **1996**, *100*, 1008.
(24) Miller, T. M.; Grassian, V. H. *J. Am. Chem. Soc.* **1995**, *117*, 10969. *Appl. Spec.* **1988**, *42*, 674.
(25) Aris, R. *The Mathematical Theory of Diffusion and Reaction in Permeable Catalysts*; Clarendon Press: Oxford, 1975.
(26) Keyser, L. F.; Moore, S. B.; Leu, M.-T. *J. Phys. Chem.* **1991**, *95*, 5496.
(27) Lide, D. R. *CRC Handbook of Chemistry and Physics*, 72nd ed.; CRC Press: Boca Raton, FL, 1991; pp 4−50.
(28) Underwood, G. M.; Li, P.; Usher, C. R.; Grassian, V. H. *J. Phys. Chem. A.* **2000**, *104*, 819.
(29) Atkins, P. A. *Physical Chemistry*, 6th ed.; W. H. Freeman and Co.: New York, 1998; p.753.
(30) Jacox, M. E. *J. Phys. Chem. Ref. Data*. **1990**, *19*, 1444.
(31) Kirchner, V.; Scheer, V.; Vogt, R. *J. Phys. Chem. A* **2000**, *104*, 8908.